JOC The Journal of Organic Chemistry

Article

pubs.acs.org/joc

Aphadilactones A–D, Four Diterpenoid Dimers with DGAT Inhibitory and Antimalarial Activities from a Meliaceae Plant

Jia Liu,[†] Xiu-Feng He,[†] Gai-Hong Wang,[†] Emilio F. Merino,[‡] Sheng-Ping Yang,[†] Rong-Xiu Zhu,[∥] Li-She Gan,[⊥] Hua Zhang,[†] Maria B. Cassera,[‡] He-Yao Wang,[†] David G. I. Kingston,[§] and Jian-Min Yue*[,†]

[†]State Key Laboratory of Drug Research, Shanghai Institute of Materia Medica, Chinese Academy of Sciences, 555 Zu Chong Zhi Road, Shanghai 201203, P. R. China

[‡]Department of Biochemistry and the Virginia Tech Center for Drug Discovery, MC 0308, Virginia Polytechnic Institute and State University, Blacksburg, Virginia 24061, United States

[§]Department of Chemistry and the Virginia Tech Center for Drug Discovery, MC 0212, Virginia Polytechnic Institute and State University, Blacksburg, Virginia 24061, United States

[∥]School of Chemistry and Chemical Engineering, Shandong University, Jinan 250100, P. R. China

[⊥]College of Pharmaceutical Sciences, Zhejiang University, Hangzhou 310058, P. R. China

Supporting Information

ABSTRACT: Aphadilactones A–D (**1**–**4**), four diastereoisomers possessing an unprecedented carbon skeleton, were isolated from the Meliaceae plant *Aphanamixis grandifolia*. Their challenging structures and absolute configurations were determined by a combination of spectroscopic data, chemical degradation, fragment synthesis, experimental CD spectra, and ECD calculations. Aphadilactone C (**3**) with the 5*S*,11*S*,5′*S*,11′*S* configuration showed potent and selective inhibition against the diacylglycerol *O*-acyltransferase-1 (DGAT-1) enzyme (IC_{50} = 0.46 ± 0.09 μM, selectivity index > 217) and is the strongest natural DGAT-1 inhibitor discovered to date. In addition, compounds **1**–**4** showed significant antimalarial activities with IC_{50} values of 190 ± 60, 1350 ± 150, 170 ± 10, and 120 ± 50 nM, respectively.

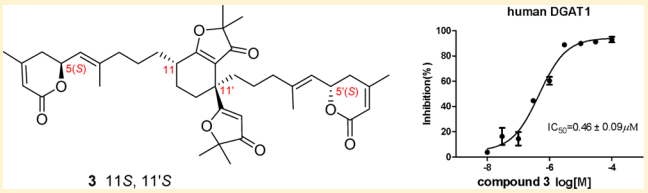

INTRODUCTION

Excessive triglyceride accumulation in adipocytes is associated with a number of human diseases such as obesity, diabetes, and steatohepatitis (fatty liver disease). Two diacylglycerol *O*-acyltransferase (DGAT) isozymes, DGAT-1 and DGAT-2, have been reported to play important roles in triglyceride synthesis and metabolism.[1] DGAT-1-deficient mice are resistant to diet-induced obesity and have decreased adiposity and improved insulin and leptin sensitivity. In contrast, newborn DGAT-2-deficient mice are lipopenic and die soon after birth.[2] Selective inhibition of DGAT-1 therefore represents a novel and potential approach for the treatment of obesity, dyslipidemia, and metabolic syndrome.[2] A number of natural DGAT-1 inhibitors have been discovered in the past decade from both plants and microbes, and the five most potent natural inhibitors show IC_{50} values ranging from 2.5 to 9.8 μM.[2,3]

In our search for new classes of potent and selective DGAT inhibitors, the plant *Aphanamixis grandifolia* (Meliaceae) came to our attention, as one of the fractions from its ethanolic extract exhibited significant inhibition against DGAT-1. *A. grandifolia*, an arbor tree, grows mainly in the tropical and subtropical areas of Asia,[4] and its leaves and roots have been used as folk medicine in China to treat rheumatism and alleviate pain.[5] Previous chemical studies on this plant afforded sesquiterpenoids,[6] triterpenoids,[7] and limonoids,[8] but none of them were reported to have activity against DGAT or DGAT-associated diseases. The DGAT-1 inhibitory fraction was thus subjected to extensive fractionation and purification to obtain four major stereoisomers, aphadilactones A–D (**1**–**4**) (Figure 1), whose carbon skeleton represents a new structure class. Further biological tests of the pure compounds **1**–**4** verified

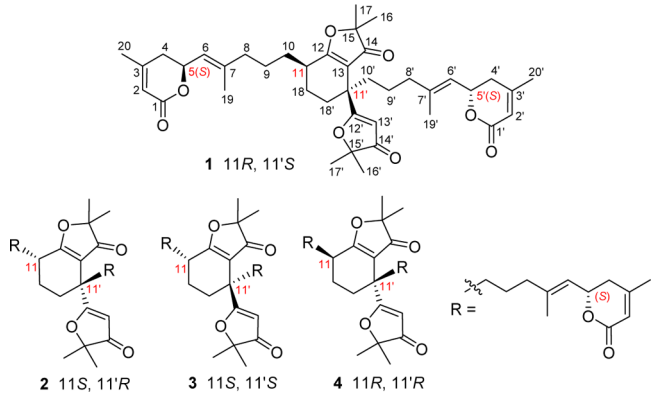

Figure 1. Structures of compounds **1**–**4**.

Received: October 23, 2013
Published: December 17, 2013

Table 1. ^{1}H NMR Data [δ_H (mult, J in Hz)] for 1−8 in CD_3OD

proton	1[a]	2[b]	3[b]	4[b]	5 (6)[b]	7 (8)[b]
2	5.79 (m)	5.79 (br s)	5.78 (br s)	5.78 (br s)		
4a	2.35 (dd, 18.0, 4.3)	2.38 (m)	2.35 (dd, 18.2, 4.7)	2.37 (m)		
4b	2.43 (dd, 18.0, 10.9)	2.45 (dd, 18.1, 10.2)	2.44 (m)	2.44 (m)		
5	5.21 (m)	5.22 (m)	5.23 (m)	5.23 (m)		
6	5.35 (br d, 8.5)	5.36 (br d, 8.1)	5.39 (br d, 8.6)	5.39 (br d, 8.6)		
8	2.09 (m, 2H)	2.10 (m, 2H)	2.14 (br t, 7.1, 2H)	2.14 (m, 2H)	2.52 (m, 2H)	2.56 (m, 2H)
9	1.53 (m, 2H)	1.53 (m, 2H)	1.63 (m, 2H)	1.63 (m, 2H)	1.61 (m, 2H)	1.70 (m, 2H)
10a	1.54 (m)	1.53 (m)	1.56 (m)	1.60 (m)	1.47 (m)	1.53 (m)
10b	1.76 (m)	1.79 (m)	1.78 (m)	1.76 (m)	1.77 (m)	1.76 (m)
11	2.74 (m)	2.75 (m)	2.64 (m)	2.64 (m)	2.70 (m)	2.61 (m)
16	1.38 (s, 3H)[c]	1.38 (s, 3H)[c]	1.37 (s, 3H)	1.37 (s, 3H)[c]	1.37 (s, 3H)[c]	1.36 (s, 3H)[c]
17	1.39 (s, 3H)[c]	1.39 (s, 3H)[c]	1.37 (s, 3H)	1.38 (s, 3H)[c]	1.38 (s, 3H)[c]	1.37 (s, 3H)[c]
18α	2.03 (m)	1.48 (m)	1.92 (m)	1.82 (m)	2.04 (m)[e]	1.92 (m)[e]
18β	1.48 (m)	2.05 (m)	1.82 (m)	1.92 (m)	1.50 (m)[e]	1.82 (m)[e]
19	1.73 (d, 0.8, 3H)	1.73 (br s, 3H)	1.76 (d, 1.3, 3H)	1.76 (d, 1.2, 3H)	2.11 (s, 3H)	2.15 (s, 3H)
20	2.02 (br s, 3H)	2.02 (br s, 3H)	2.02 (br s, 3H)	2.02 (br s, 3H)		
2′	5.79 (br s)	5.79 (br s)	5.78 (br s)	5.78 (br s)		
4′a	2.34 (dd, 18.0, 4.2)	2.34 (dd, 18.1, 4.4)	2.34 (dd, 18.2, 4.7)	2.34 (dd, 18.1, 4.5)		
4′b	2.43 (dd, 18.0, 10.9)	2.45 (dd, 18.1, 10.2)	2.42 (m)	2.44 (m)		
5′	5.21 (m)	5.20 (m)	5.21 (m)	5.21 (m)		
6′	5.33 (br d, 8.5)	5.34 (br d, 8.2)	5.32 (br d, 8.6)	5.35 (br d, 8.6)		
8′	2.06 (m, 2H)	2.06 (m, 2H)	2.07 (br t, 7.4, 2H)	2.09 (m, 2H)	2.48 (m, 2H)	2.50 (m, 2H)
9′a	1.29 (m)	1.24 (m)	1.35 (m)	1.33 (m)	1.34 (m)	1.43 (m)
9′b	1.50 (m)	1.50 (m)	1.47 (m)	1.46 (m)	1.59 (m)	1.56 (m)
10′a	1.89 (ddd, 13.0, 13.0, 4.4)	1.82 (m)	1.87 (m)	1.84 (m)	1.89 (m)	1.86 (m)
10′b	2.09 (m)	2.16 (m)	2.03 (m)	2.05 (m)	2.07 (m)	1.99 (ddd, 13.0, 13.0, 4.5)
13′	5.29 (s)	5.27 (s)	5.34 (s)	5.33 (s)	5.31 (s)	5.41 (s)
16′	1.33 (s, 3H)[d]	1.33 (s, 3H)[d]	1.31 (s, 3H)[d]	1.31 (s, 3H)[d]	1.32 (s, 3H)[d]	1.30 (s, 3H)[d]
17′	1.36 (s, 3H)[d]	1.36 (s, 3H)[d]	1.35 (s, 3H)[d]	1.35 (s, 3H)[d]	1.35 (s, 3H)[d]	1.34 (s, 3H)[d]
18′α	1.82 (ddd, 13.4, 13.4, 2.7)	2.07 (m)	1.92 (m)	1.92 (m)	1.84 (m)[e]	1.92 (m)
18′β	2.11 (m)	1.86 (m)	1.92 (m)	1.92 (m)	2.09 (m)[e]	1.92 (m)
19′	1.71 (d, 0.7, 3H)	1.69 (br s, 3H)	1.71 (d, 1.2, 3H)	1.68 (d, 1.2, 3H)	2.13 (s, 3H)	2.11 (s, 3H)
20′	2.02 (br s, 3H)	2.01 (br s, 3H)	2.02 (br s, 3H)	2.02 (br s, 3H)		

[a]Recorded at 700 MHz. [b]Recorded at 400 MHz. [c,d]May be exchanged in the same column. [e]The relative configurations of H-18 and H-18′ assigned for **5** and **7** were reversed in **6** and **8** vertically.

that aphadilactone C (**3**) is the primary active component, with potent inhibition against DGAT-1 (IC_{50} = 0.46 ± 0.09 μM) but only marginal activity against DGAT-2 (IC_{50} > 100 μM), indicating that it is a highly selective DGAT-1 inhibitor with a selectivity index of >217. Most excitingly, aphadilactone C is the strongest natural DGAT-1 inhibitor discovered to date, being >5-fold more active than the best previously reported one, erysenegalensein O (IC_{50} = 2.5 μM).[3b]

Another pharmacological activity screening for **1**−**4** showed that they are also active against *Plasmodium falciparum* in vitro culture, with IC_{50} values of 190 ± 60, 1350 ± 150, 170 ± 10, and 120 ± 50 nM, respectively. Malaria is caused by protozoan parasites of the *Plasmodium* genus, of which *P. falciparum* is responsible for most of the fatal cases. The parasite is transmitted between human hosts by *Anopheles* mosquitoes. It is widespread in tropical and subtropical regions, including parts of America, Asia, and Africa. Malaria has infected humans for over 50 000 years, and it continues to cause about 200−300 million cases and kills nearly a million people annually in Africa alone.[9] Historically, plants have been a prominent source of antimalarial drugs such as quinine and artemisinin.[10] Artemisinin combination therapies are recommended by the World Health Organization as the first-line treatment for malaria and are extremely safe and effective after 3 days of dosing.[11] However, given the emergence of resistance to artemisinin and other antimalarials, the need for new medicines is ever present.[12] *P. falciparum* encodes only one DGAT enzyme, which is essential for intraerythrocytic proliferation.[13] Infected erythrocytes display a dramatic increase in triglyceride content; however, *P. falciparum* lacks the capability to degrade triglycerides to produce energy, and instead, triglycerides are part of the lipid bodies in the food vacuole.[14]

We present herein the isolation, structural elucidation, and biological activities of **1**−**4** along with a brief structure−activity relationship (SAR) discussion of this compound class.

RESULTS AND DISCUSSION

Aphadilactone A (**1**) was obtained as a pale gum with $[\alpha]_D^{22}$ −8.3 (*c* 0.145, MeOH). The molecular formula, $C_{40}H_{52}O_8$ with 15 degrees of unsaturation, was determined by HR-ESI-MS(+), which showed a peak at *m*/*z* 683.3569 $[M + Na]^+$ (calcd 683.3560). Its IR spectrum displayed absorptions of carbonyl (1699 cm^{-1}) and double bond (1606 cm^{-1}) functionalities. In accord with the molecular formula, 40 carbon signals were resolved in its ^{13}C NMR spectrum (Table 2), including eight methyls, 10 sp^3 methylenes, eight methines (two oxygenated and five olefinic), and 14 quaternary carbons (two oxygenated, five olefinic, and six carbonyl), as distinguished by DEPT

dx.doi.org/10.1021/jo402340h | J. Org. Chem. 2014, 79, 599−607

experiments in combination with HSQC and HMBC spectra [S9 and S10 in the Supporting Information (SI)]. Overall analysis of the NMR data (Tables 1 and 2) further indicated the presence of furan-3(2*H*)-one and *α,β*-unsaturated *δ*-lactone moieties,[15] which was supported by the UV absorption at λ_{max} = 265 nm.

Table 2. ^{13}C NMR Data for 1−8 in CD_3OD

carbon	1[b]	2[a]	3[a]	4[a]	5 (6)[b]	7 (8)[b]
1	168.1	168.0	167.9	167.9		
2	116.4	116.4	116.5	116.4		
3	161.2	161.2	161.1	161.1		
4	35.8	35.7	35.8	35.8		
5	76.0	75.9	76.0	76.0		
6	123.6	123.7	123.9	123.8		
7	143.6	143.5	143.4	143.5	211.3	211.4
8	40.2	40.2	40.0	40.1	43.9	43.8
9	25.0	24.9	25.9	25.9	21.4	22.2
10	31.2	31.1	32.1	32.1	31.3	32.2
11	37.7	37.6	36.5	36.6	37.7	36.8
12	193.1	193.2	193.1	193.1	193.0	193.1
13	112.4	112.3	112.1	112.0	112.2	112.0
14	206.9	206.8	206.6	206.6	206.9	206.8
15	89.4	89.4	89.2	89.2	89.5	89.3
16	23.1[c]	23.1[c]	23.1[c]	23.1[c]	23.0[c]	23.1[c]
17	23.4[c]	23.4[c]	23.5[c]	23.4[c]	23.3[c]	23.3[c]
18	25.9	25.9	24.9	24.8	25.8	24.7
19	16.7	16.6	16.6	16.6	29.8	29.8
20	23.0	23.0	23.0	23.0		
1′	168.1	168.0	167.9	167.9		
2′	116.4	116.4	116.5	116.5		
3′	161.2	161.2	161.1	161.2		
4′	35.8	35.8	35.8	35.8		
5′	76.0	76.0	76.0	76.0		
6′	123.6	123.9	123.6	124.0		
7′	143.5	143.4	143.4	143.3	211.3	211.3
8′	40.4	40.5	40.4	40.5	44.2	44.1
9′	23.4	23.2	23.7	23.6	19.6	20.0
10′	35.6	35.2	35.8	35.6	35.4	35.7
11′	43.5	43.4	43.1	43.1	43.4	43.1
12′	197.9	198.0	197.5	197.6	197.7	197.4
13′	102.2	102.2	101.9	101.9	102.2	102.0
14′	209.8	209.7	209.8	209.9	209.8	210.1
15′	90.6	90.5	90.3	90.5	90.5	90.3
16′	23.0	23.0	23.0	23.0	22.9	22.9
17′	23.0	23.0	23.0	23.0	22.9	22.9
18′	31.6	31.5	30.4	30.5	31.4	30.4
19′	16.6	16.5	16.8	16.5	29.9	29.9
20′	23.0	23.0	23.0	23.0		

[a]Recorded at 100 MHz. [b]Recorded at 125 MHz. [c]May be interchangeable in the same column.

The ^{1}H−^{1}H COSY and HSQC spectra of **1** revealed four proton-bearing structural fragments: C-4 to C-6; C-8 to C-11, C-18, and C-18′; C-4′ to C-6′; and C-8′ to C-10′ (shown as bold bonds in Figure 2). The connections of these fragments with the other functional groups of **1** were mainly determined by analysis of the HMBC spectrum (Figure 2). The carbon chemical shifts and the HMBCs of H-20 with C-2 (δ_C 116.4), C-3 (δ_C 161.2), and C-4 and of H-2 with C-1 (δ_C 168.1) indicated the presence of an *α,β*-unsaturated carbonyl group linked to C-4 via the C-3/C-4 bond as well as the attachment of

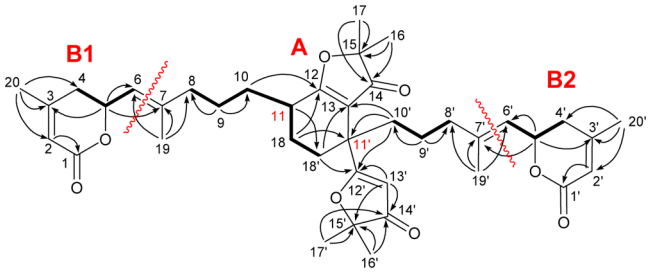

Figure 2. ^{1}H−^{1}H COSY (bold bonds) and H → C HMBC correlations (arrows) in **1**.

C-20 to C-3. The deshielded resonance of H-5 (δ_H 5.21) suggested the formation of a six-membered lactone between C-1 and C-5 to furnish a 4,6-dimethyl-5,6-dihydro-2*H*-pyran-2-one motif (component B1). In the same way, an identical component B2 (C-1′ to C-6′ and C-20′) was readily established. The chemical shifts of C-12 (δ_C 193.1), C-13 (δ_C 112.4), and C-14 (δ_C 206.9) were suggestive of an *α,β*-unsaturated ketone moiety, and its C-14 end was shown to be connected to C-15 (δ_C 89.4) bearing two methyls by the HMBCs of H-16 and H-17 with C-14 and C-15. This analysis together with the deshielded resonances of C-12 and C-15 indicated the presence of a 2,2-dimethylfuran-3(2*H*)-one subunit (C-12 to C-17).[15] Similarly, another 2,2-dimethylfuran-3(2*H*)-one subunit (C-12′ to C-17′) was constructed on the basis of chemical shifts and HMBCs (Figure 2). C-12 was shown to be linked to C-11 by the HMBCs of H-10 and H-18 with C-12. The HMBCs of H-18 with C-11′, H-18′ with C-13 and C-12′, and H-10′ with C-13, C-11′, and C-12′ showed that C-13, C-10′, and C-12′ are attached to C-11′ to fix a cyclohexene ring. The HMBCs of H-19 with C-6, C-7, and C-8 and H-19′ with C-6′, C-7′, and C-8′ revealed the linkages of C-8 and C-19 to C-7 and C-8′ and C-19′ to C-7′, respectively, to construct component A and also enabled us to fix the Δ-6 and Δ-6′ double bonds, which were confirmed by the HMBCs of H-5 with C-6 and C-7 and H-5′ with C-6′ and C-7′, respectively. The planar structure of **1** was thus established, and it was secured by spectral analysis of its ozonized products,[16] compounds **5** and **9** (Figure 3 and Figure S1 in the SI).

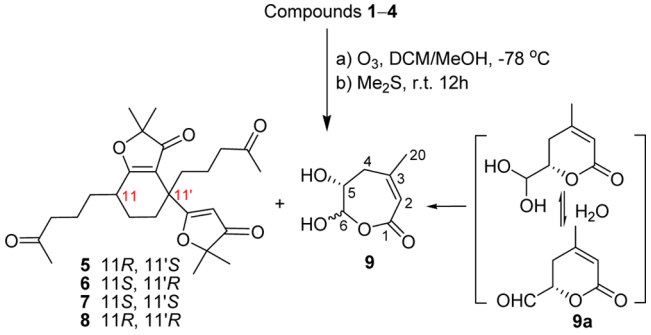

Figure 3. Ozonolysis of compounds **1**−**4**.

The ESI-MS, UV, IR, and ^{1}H and ^{13}C NMR (Tables 1 and 2) data for compounds **2**−**4** showed high similarities to those of **1**, and the minor variations were the proton and carbon resonances around the cyclohexene ring. It was also obvious that the NMR data for **1** and **2** were very similar, as were those for **3** and **4**. These data suggested that these compounds were

dx.doi.org/10.1021/jo402340h | J. Org. Chem. 2014, 79, 599−607

four stereoisomers with different configurations at C-11 and C-11′. Comprehensive spectral analysis (Tables 1 and 2 and SI S12−S41), especially of the 2D NMR spectra, verified that **2**−**4** possess the same planar structure as **1** (Figure 1).

The NOESY correlations of H-6 with H-8 and H-6′ with H-8′ revealed that both the Δ-6 and Δ-6′ double bonds of **1**−**4** have the *E* geometry. In the NOESY spectrum of **1** (Figure 4

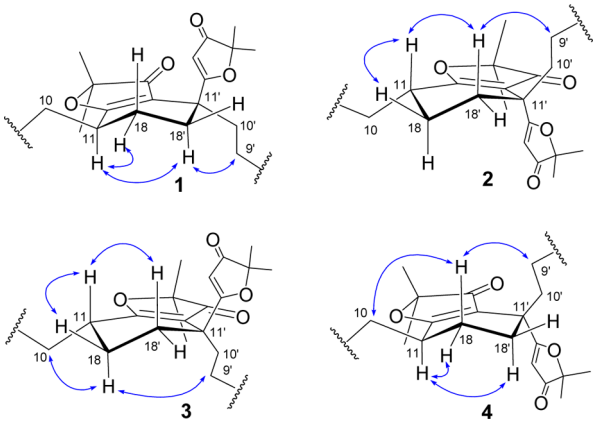

Figure 4. Key NOESY correlations (blue arrows) in **1**−**4**.

and SI S11), the strong correlation of H-11 with H-18′α indicated that they adopt 1,3-diaxial positions in the half-chair cyclohexene ring, and they were arbitrarily fixed as α-oriented, which was supported by the coupling constants of H-18′α at δ_H 1.82 [ddd, 13.4 (geminal), 13.4 (ax−ax), and 2.7 (ax−eq) Hz]. Consequently, the long chain at C-11′ of **1** was assigned as α-directed by the key correlation of H-9′b with H-18′α (SI S11; see the expanded parts). Thus, the two wings incorporating lactone rings at C-11 and C-11′ of the cyclohexene ring in **1** were definitely assigned as *trans*-oriented, and this was confirmed by the strong NOESY correlations of H-11 and H-9′b with H-18′α observed for its ozonized product **5** (SI S51). Similarly, the relative configurations at C-11 and C-11′ of **2** were assigned as depicted by the key NOESY correlations of H-11 and H-9′b with H-18′β (Figure 4 and SI S21). In a similar fashion, the two wings at C-11 and C-11′ in **3** and **4** were determined to be *cis*-oriented in the half-chair cyclohexene ring by the key NOESY correlations (Figure 4) observed for **3** (H-11 with H-18′β and H-18α with H-9b′; SI S31) and **4** (H-11 with H-18′α and H-18β with H-9b′; SI S41). The mirror-image CD spectra of the ozonized products (**5**/**6** and **7**/**8**) (Figure 5) rigorously support the assignments of the relative configurations of C-11 and C-11′ in **1**−**4**.

The CD spectra of **1**−**4** (Figure S2 in the SI) result from the interactions of the multiple chromophores and did not provide useful Cotton effects (CEs) for the assignment of absolute stereochemistry. Fortunately, the typical CD curves of their correspondingly ozonized products **5**−**8** representing two pairs of enantiomers (**5**/**6** and **7**/**8**) allowed the absolute configurations at C-11 and C-11′ of the molecules to be established (Figure 5).[17] The CD exciton couplets of **5**−**8** associated with the two chromophores of the 2,2-dimethylfuran-3(2*H*)-one moieties[15] (centered at ca. λ_{max} = 264 nm) were observed. The clear first negative CE (λ = 274 nm) and the second positive CE (λ = 239 nm) of **7** (ozonized from **3**) showed a negative helicity between two chromophores, establishing an 11*S*,11′*S* configuration for compounds **3** and **7**. Consequently, the opposite CD curves (positive CE at 274

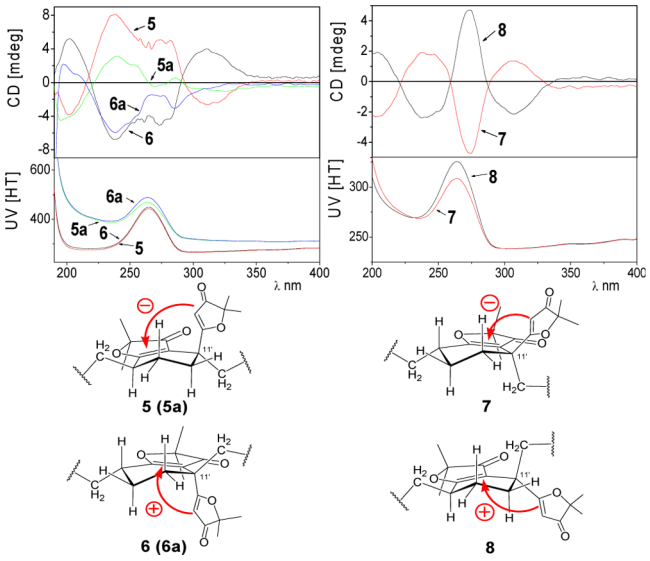

Figure 5. Experimental ECD spectra of **5**−**8**, **5a**, and **6a**.

nm, negative CE at 238 nm) of **8** (ozonized from **4**) indicated that **4** and **8** have an 11*R*,11′*R* configuration. While **5** (ozonized from **1**) exhibited an obvious positive CE at 239 nm arising from exciton coupling of the two chromophores, a negative CE at ca. 274 nm expected by comparison to those of **7** and **8** was eclipsed for unspecified reasons. To remove the ambiguity and the interactions among the multiple chromophores, **5** was reduced with $NaBH_4$ in CH_3OH to afford its diol derivative **5a** (Figure 6), which showed a first negative CE

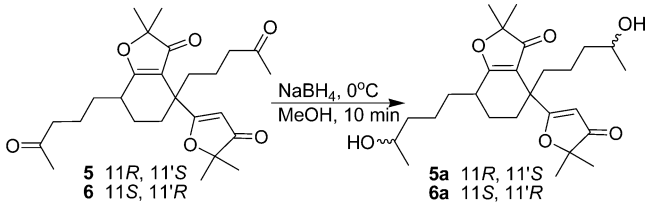

Figure 6. Reduction of compounds **5** and **6**.

(weak, λ = 270 nm) and a second positive CE (λ = 240 nm), suggestive of a negative helicity between the two chromophores, indicating that **1**, **5**, and **5a** have the 11*R*,11′*S* configuration. The opposite CD curves of **6** (ozonized from **2**) and **6a** versus those of **5** and **5a** thus revealed the reversed configuration (11*S*,11′*R*) for **2**, **6**, and **6a**. ECD calculations for compounds **5**−**8** matched the experimental data well (Figure 7), which further confirmed the above assignments.

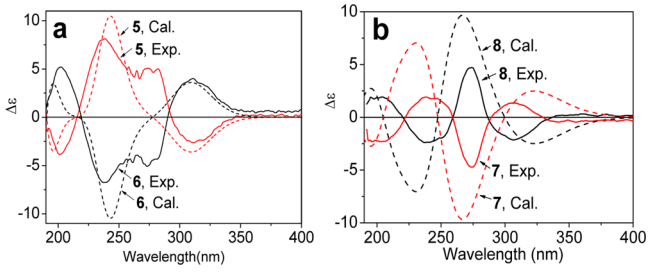

Figure 7. Calculated ECD spectra of compounds **5**−**8** vs the experimental ECD curves: (a) **5** and **6**; (b) **8** and **7**.

dx.doi.org/10.1021/jo402340h | *J. Org. Chem.* 2014, 79, 599−607

The configurational assignment of the lactone rings of **1**–**4** was much more challenging because of their remote locations from the central core of the molecules. Ozonolysis of **1** (or **2**–**4**) afforded **9** in low yields as an inseparable mixture of two epimers instead of the expected aldehyde (**9a**), likely as a result of the unstable nature of **9a** in the presence of H_2O or the excess of ozone that may have further decomposed **9** or **9a** (Figure 3). In order to define the absolute configurations at C-5 and C-5′ in **1**–**4**, two model compounds **13** and **14** with *S* and *R* configurations, respectively, were synthesized from the starting materials (*R*)- and (*S*)-oxiran-2-ylmethanol, respectively (Figure 8).[18] With **13** and **14** in hand, an alternative

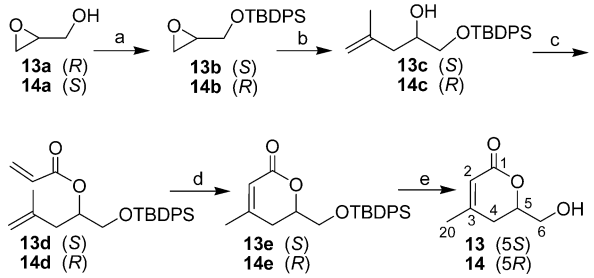

Figure 8. Syntheses of **13** and **14**. Reagents and conditions: (a) TBDPSiCl, imidazole, DMF; (b) CuI, $CH_3CH(CH_2)MgBr$, THF, −30 to 0 °C; (c) $CH_2CHCOCl$, Et_3N, DMAP, CH_2Cl_2, 0 °C; (d) Grubbs' catalyst II, CH_2Cl_2, 50 °C; (e) Bu_4NF, THF.

strategy aiming to obtain **13** and/or **14** from **1**–**4** under mild conditions was thus designed (Figure 9); we expected that if C-5 and C-5′ bore different absolute configurations, they could be distinguished by oxidative degradation of the partially dihydroxylated products **10a** and **11a**. Fortunately, after dihydroxylation with potassium osmate,[19] compound **1** gave the three products **10a**–**12a** in isolated yields of 13–15%, as expected. Each of these was further oxidized with $Pb(OAc)_4$[20] and then reduced with $NaBH_4$,[21] and the resulting reaction mixtures were directly subjected to chiral HPLC analysis. One HPLC peak at ca. t_R = 13.9 min in the degraded products of **10a**–**12a** matched that of the authentic sample **13** (Figure S3 in the SI), and no peak corresponding to **14** was observed, indicating that both C-5 and C-5′ of **1** have the *S* configuration. Similarly, **2**–**4** separately underwent the cascade of dihydroxylation, oxidation, and reduction in a one-pot reaction, and each reaction mixture was analyzed by chiral HPLC (Figure S4 in the SI), which revealed that C-5 and C-5′ in **2**–**4** are also *S*-configured. The structures of **1**–**4** were thus fully determined as shown in Figure 1.

Aphadilactones A–D are proposed to be formed from two molecules of nemoralisin-type diterpenoid **i**, enzyme-catalyzed Diels–Alder reaction of which would give the key intermediate **ii**. Compounds **1**–**4** would finally be produced from **ii** via a typical 1,3-hydrogen migration (Figure 10). This hypothesis

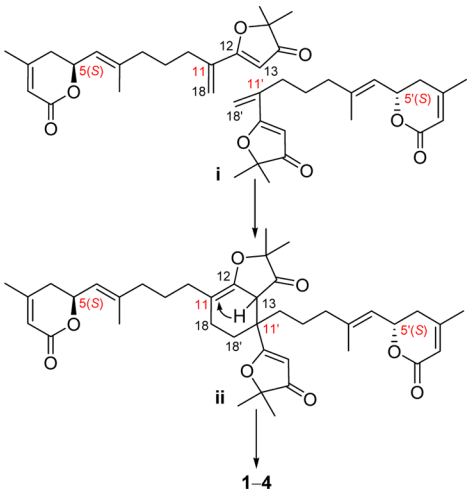

Figure 10. Plausible biosynthetic pathway for **1**–**4**.

was confirmed to be plausible by the simultaneous isolation of nemoralisin[22] in this investigation; its absolute structure was established in this study by single-crystal X-ray diffraction analysis of its derivative **15** (Figure 11 and Table S3 in the SI). Compound **15** was obtained by dihydroxylation of nemoralisin with the AD-mix-α reagent.

A review of the literature showed that the structures of **1**–**4** are biosynthetically related to those of aphanamenes A and B from the same species, which were reported by Kong and coworkers in a very recent paper.[23] Although **1**–**4** could originate from a similar or the same monomer as aphanamenes A and B, their carbon framework is different from that in the latter two compounds. Moreover, peak splitting was observed for the

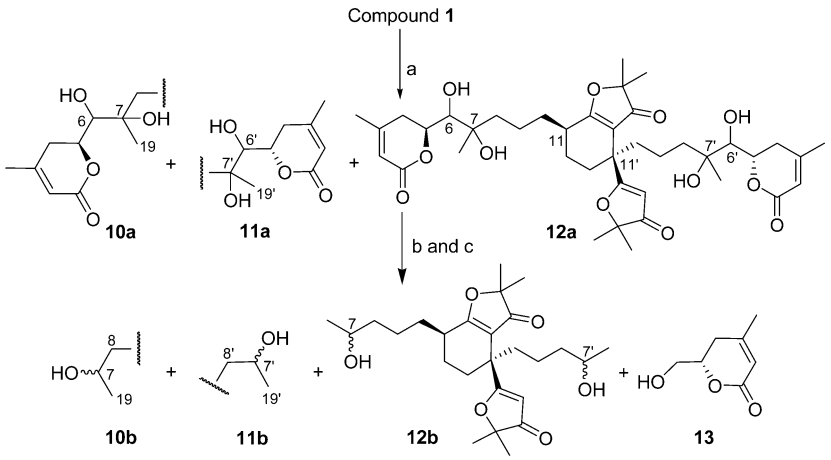

Figure 9. Oxidative degradation of **1**. Reagents and conditions: (a) 5 mol % $K_2OsO_4{\cdot}2H_2O$, 5 equiv of $MeSO_2NH_2$, 15 equiv of $K_3Fe(CN)_6$, 15 equiv of K_2CO_3, $^tBuOH/H_2O$ (1:1), r.t.; (b) $Pb(OAc)_4$, DCM, 0 °C; (c) $NaBH_4$, MeOH.

dx.doi.org/10.1021/jo402340h | J. Org. Chem. 2014, 79, 599–607

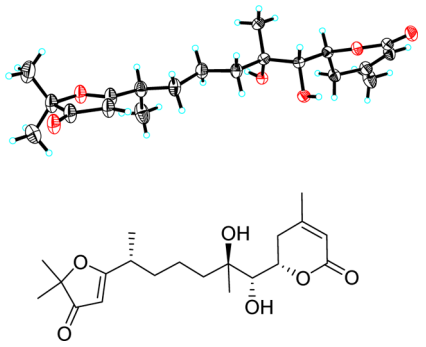

Figure 11. Single-crystal X-ray structure of compound **15**.

NMR data of aphanamene B, which was assumed by the authors to be caused by cyclohexene conformation isomerization.[23] However, on the basis of our findings that compounds **1** and **2** and compounds **3** and **4** are not separable on normal achiral HPLC columns and that the NMR "peak splitting" before further purification under chiral conditions was due to mixtures of diastereoisomers, the structure characterization of aphanamene B might need to be re-examined.

Compounds **1**−**4** and their respective ozonized products **5**−**8** were evaluated for inhibition of hDGAT enzymes. Interestingly, aphadilactone C (**3**) exhibited significant inhibitory activity against DGAT-1 with an IC_{50} of 0.46 ± 0.09 μM (SI page 14) and very weak activity against DGAT-2 (IC_{50} > 100 μM), indicating that it is a highly selective DGAT-1 inhibitor (selectivity index > 217). In this test, the natural DGAT-1 inhibitory agent betulinic acid (IC_{50} = 17.2 μM) was used as the positive control.[2] Inspection of the structures and activities of **1**−**8** against DGAT-1 at 10 μM (Table S4 in the SI) outlined a gross SAR. Compounds **1** and **3** exhibited 25.5% and 85.9% inhibitions on DGAT-1 at 10 μM, respectively, while the other analogues only showed marginal inhibitions. These results primarily indicate the following: (1) an 11′*S* configuration (as in **1** and **3**) is crucial for the activity, and the 11*S* configuration as in **3** that keeps the two lactone-containing wings away from the two furan-3(2*H*)-one moieties enhances the activity; (2) the length of the two wings, the double bonds, and the lactone rings are also important for the activity. This gross SAR analysis of these diastereoisomers indicates that the active binding site of the DGAT-1 enzyme is highly selective to the stereochemistry of the substrate.

Compounds **1**−**4** were also tested for in vitro antimalarial activity, and they exhibited significant activities with IC_{50} values of 190 ± 60, 1350 ± 150, 170 ± 10, and 120 ± 50 nM, respectively. Artemisinin was used as the positive control, and its IC_{50} value was 7.3 ± 0.3 nM (Table 3). Further studies are required in order to establish whether their mechanism of action involves inhibition of PfDGAT enzyme.

CONCLUSION

Our chemical investigation into the Chinese herb *A. grandifolia* has led to the isolation of a new class of diterpenoid dimers, aphadilactones A−D (**1**−**4**). Compound **3** showed very potent and selective inhibition against DGAT-1 (IC_{50} = 0.46 ± 0.09 μM, selectivity index > 217) whereas its stereoisomers **1**, **2**, and **4** showed only marginal inhibitions, suggesting that stereospecific binding between DGAT-1 enzyme and its inhibitors is required. Interestingly, compound **2** showed the weakest activity against *P. falciparum*, while **1**, **3**, and **4** were more potent. Our study also revealed a gross SAR of DGAT-1 inhibition for this compound class, which will be important for the structural optimization. To the best of our knowledge, aphadilactone C (**3**) is the strongest natural DGAT-1 inhibitor discovered to date,[2,3] and it represents a new structural scaffold for DGAT inhibitors and highlights the potential for future structural optimization and/or total synthesis. We view aphadilactone C as a promising new class of DGAT-1 inhibitor that deserves further investigation. The strong antimalarial activities of **1**, **3**, and **4** also make them promising candidates for antimalarial drugs. This finding once again demonstrates the robust capability of nature to produce stereochemically diverse molecules that are a precious treasure for drug discovery.

EXPERIMENTAL SECTION

General Experimental Procedures. IR spectra were recorded with KBr disks. Optical rotations were measured at room temperature. NMR spectra were mainly measured on a 400 or 500 MHz spectrometer, except for the NOESY spectra, which were measured on a 700 MHz spectrometer. HR-ESI-MS was carried out on a TOF mass spectrometer. EI-MS spectra were measured on a spectrometer by direct inlet at 70 eV. An ODS-A column (10 mm × 250 mm, S-5 μm, 12 nm) and an AD-H column (10 mm × 250 mm, 5 μm) were used for the semipreparative HPLC analysis. Data collections for crystal structure analysis were performed at room temperature (293 K) employing graphite-monochromatized Cu Kα radiation (λ = 1.54178 Å).

Plant Material. The leaves of *A. grandifolia* BL were collected from Sanya of Hainan Island, People's Republic of China, in May 2010 and were identified by Prof. Shi-Man Huang (Department of Biology, Hainan University, P. R. China). A voucher specimen has been deposited with the Shanghai Institute of Materia Medica, Chinese Academy of Sciences, P. R. China (accession number AP-2010-2Y).

Extraction and Isolation. The dried powder of the leaves of *A. grandifolia* (5 kg) was extracted three times with 95% ethanol at room temperature to give a crude extract (350 g), which was then partitioned between EtOAc and water to yield an EtOAc-soluble fraction E (150 g). Fraction E was subjected to a column of MCI gel ($MeOH/H_2O$, 50:50−90:10 v/v) to give four fractions E1−E4. Fraction E3 (13.3 g) showed significant inhibition (ca. 41%, 10 μg/mL) on DGAT-1 enzyme and was subjected to column chromatography using reversed-phase C18 silica gel ($MeOH/H_2O$, 65:35−85:15 v/v) to obtain the major fraction E3a, which mainly contained aphadilactones A−D (553 mg). Fraction E3a was further separated by semipreparative HPLC equipped with a C18 silica gel column (10 mm × 250 mm, YMC Co., Ltd.) and eluted with the mobile phase of CH_3CN/H_2O (68:32 v/v) to afford two fractions, E3a1 (260 mg) and E3a2 (228 mg). Each of the fractions E3a1 and E3a2 showed a homogeneous single peak in HPLC analysis (C18 silica gel column, even run under a number of optimized conditions) but displayed very complicated NMR characteristics suggestive of a mixture. Fraction E3a1 was thus subjected to a further purification by semipreparative HPLC using a chiral AD-H column (10 mm × 250 mm, Daicel Chemical Industries, Ltd.) with *n*-hexane/isopropanol/ethanol (70:10:20 v/v) as the mobile phase to yield compounds **1** (126 mg) and **2** (100 mg). In the same way, fraction E3a2 afforded **3** (120 mg) and **4** (55 mg).

Table 3. Antimalarial (*P. falciparum*) Activities of Compounds 1−4 in Vitro

compound	**1**	**2**	**3**	**4**	artemisinin
IC_{50} (nM)	190 ± 60	1350 ± 150	170 ± 10	120 ± 50	7.3 ± 0.3

dx.doi.org/10.1021/jo402340h | *J. Org. Chem.* 2014, 79, 599−607

Compounds **1**−**4** were confirmed to exist in the ethanolic crude extract of the leaves by both TLC (four compounds showed the same R_f = 0.6 in chloroform/MeOH, 20:1) and HPLC (t_R = 14.8 min for **1** and **2**, t_R = 13.2 min for **3** and **4**; C-18 column with a mobile phase of CH_3CN/H_2O, 70:30 v/v).

Aphadilactone A (1). Pale gum; $[\alpha]_D^{22}$ −8.3 (*c* 0.145, MeOH); ^1H and ^{13}C spectroscopic data, see Tables 1 and 2; IR (KBr) ν_{max} 2931, 1699, 1606, 1574, 1415, 1381, 1246, 1174, 1041, 850 cm^{-1}; UV/vis λ_{max}/nm (log ε) 265.4 (4.21); CD (MeOH) λ_{max}/nm ($\Delta\varepsilon$) 283 (2.31), 253 (−5.22), 230 (1.03); ESI-MS(+) *m*/*z* 661.5 $[M + H]^+$, 683.4 $[M + Na]^+$; ESI-MS(−) *m*/*z* 659.9 $[M - H]^-$; HR-ESI-MS(+) *m*/*z* 683.3569 $[M + Na]^+$ (calcd for $C_{40}H_{52}O_8Na$, 683.3560).

Aphadilactone B (2). Pale gum; $[\alpha]_D^{22}$ −40.7 (*c* 0.15, MeOH); ^1H and ^{13}C spectroscopic data, see Tables 1 and 2; IR (KBr) ν_{max} 2931, 1697, 1606, 1574, 1439, 1415, 1381, 1246, 1221, 1174, 1041, 850 cm^{-1}; UV/vis (MeOH) λ_{max}/nm (log ε) 265.2 (4.36); CD (MeOH) λ_{max}/nm ($\Delta\varepsilon$) 243 (−8.66), 224 (4.24); ESI-MS(+) *m*/*z* 661.5 $[M + H]^+$, 683.4 $[M + Na]^+$; ESI-MS(−) *m*/*z* 659.7 $[M - H]^-$; HR-ESI-MS(+) *m*/*z* 661.3727 $[M + H]^+$ (calcd for $C_{40}H_{53}O_8$, 661.3740).

Aphadilactone C (3). Pale gum; $[\alpha]_D^{20}$ 4.0 (*c* 0.125, MeOH); ^1H and ^{13}C spectroscopic data, see Tables 1 and 2; IR (KBr) ν_{max} 2931, 1699, 1608, 1576, 1458, 1381, 1362, 1246, 1176, 1072, 1041, 850 cm^{-1}; UV/vis (MeOH) λ_{max}/nm (log ε) 266.0 (4.08); CD (MeOH) λ_{max}/nm ($\Delta\varepsilon$) 308 (1.02), 267 (−2.28), 252 (−1.87), 230 (0.15); ESI-MS(+) *m*/*z* 661.6 $[M + H]^+$, 683.5 $[M + Na]^+$; ESI-MS(−) *m*/*z* 659.9 $[M - H]^-$; HR-ESI-MS(+) *m*/*z* 683.3561 $[M + Na]^+$ (calcd for $C_{40}H_{52}O_8Na$, 683.3560).

Aphadilactone D (4). Pale gum; $[\alpha]_D^{20}$ −15.1 (*c* 0.185, MeOH); ^1H and ^{13}C spectroscopic data, see Tables 1 and 2; IR (KBr) ν_{max} 2931, 1697, 1610, 1576, 1458, 1381, 1246, 1174, 1072, 1041, 850 cm^{-1}; UV/vis (MeOH) λ_{max}/nm (log ε) 266.0 (4.01); CD (MeOH) λ_{max}/nm ($\Delta\varepsilon$) 275 (1.49), 250 (−3.15), 224 (−1.39); ESI-MS(+) *m*/*z* 661.5 $[M + H]^+$, 683.4 $[M + Na]^+$; ESI-MS(−) *m*/*z* 659.9 $[M - H]^-$; HR-ESI-MS(+) *m*/*z* 683.3575 $[M + Na]^+$ (calcd for $C_{40}H_{52}O_8Na$, 683.3560).

Ozonolysis of Aphadilactones A−D (1−4). Compound **1** (10.0 mg, 0.015 mmol) in CH_2Cl_2/MeOH (10 mL/2 mL) was ozonized at −78 °C and then treated with dimethyl sulfide (0.2 mL).[16] The reaction mixture was allowed to warm to room temperature and stirred overnight. After workup, the resulting residue was purified by preparative TLC (developed by CH_3Cl/MeOH, 30:1 v/v) to afford 6.0 mg of compound **5** (R_f = 0.5) and 1.5 mg of compound **9** (R_f = 0.3); the latter was an inseparable mixture of two epimers. Aphadilactones B−D (**2**−**4**) (each 10.0 mg) were subjected to the same ozonolysis procedure to produce compounds **6**−**8** (6, 5, and 6 mg, respectively) compound **9** (1.0 mg) was obtained only in the ozonolysis of compound **4**.

Compound 5. Pale gum; $[\alpha]_D^{22}$ 25.7 (*c* 0.175, MeOH); ^1H and ^{13}C spectroscopic data, see Tables 1 and 2; IR (KBr) ν_{max} 2931, 1699, 1608, 1576, 1456, 1414, 1377, 1362, 1221, 1174, 937 cm^{-1}; UV/vis (MeOH) λ_{max}/nm (log ε) 264.8 (4.16); CD (MeOH) λ_{max}/nm ($\Delta\varepsilon$) 274 (1.95), 239 (3.12); ESI-MS(+) *m*/*z* 445.4 $[M + H]^+$, 467.3 $[M + Na]^+$, 911.6 $[2M + Na]^+$; ESI-MS(−) *m*/*z* 443.4 $[M - H]^-$; HR-ESI-MS(+) *m*/*z* 445.2591 $[M + H]^+$ (calcd for $C_{26}H_{37}O_6$, 445.2590).

Compound 6. Pale gum; $[\alpha]_D^{22}$ −27.8 (*c* 0.115, MeOH); ^1H and ^{13}C spectroscopic data, see Tables 1 and 2; IR (KBr) ν_{max} 2931, 1699, 1606, 1576, 1458, 1414, 1377, 1362, 1223, 1174, 937 cm^{-1}; UV/vis (MeOH) λ_{max}/nm (log ε) 265.4 (4.29); CD (MeOH) λ_{max}/nm ($\Delta\varepsilon$) 273 (−1.83), 237 (−2.42); ESI-MS(+) *m*/*z* 445.3 $[M + H]^+$, 467.2 $[M + Na]^+$, 911.6 $[2M + Na]^+$; ESI-MS(−) *m*/*z* 443.1 $[M - H]^-$; HR-ESI-MS(+) *m*/*z* 445.2588 $[M + H]^+$ (calcd for $C_{26}H_{37}O_6$, 445.2590).

Compound 7. Pale gum; $[\alpha]_D^{22}$ 40.7 (*c* 0.135, MeOH); ^1H and ^{13}C spectroscopic data, see Tables 1 and 2; IR (KBr) ν_{max} 2931, 1697, 1612, 1577, 1458, 1417, 1377, 1362, 1223, 1174, 939, 804 cm^{-1}; UV/vis (MeOH) λ_{max}/nm (log ε) 264.4 (4.17); CD (MeOH) λ_{max}/nm ($\Delta\varepsilon$) 274 (−2.12), 239 (0.86); ESI-MS(+) *m*/*z* 445.4 $[M + H]^+$, 467.4 $[M + Na]^+$, 911.6 $[2M + Na]^+$; ESI-MS(−) *m*/*z* 443.4 $[M - H]^-$; HR-ESI-MS(+) *m*/*z* 445.2590 $[M + H]^+$ (calcd for $C_{26}H_{37}O_6$, 445.2590).

Compound 8. Pale gum; $[\alpha]_D^{22}$ −42.5 (*c* 0.12, MeOH); ^1H and ^{13}C spectroscopic data, see Tables 1 and 2; IR (KBr) ν_{max} 2931, 1701, 1612, 1577, 1458, 1415, 1377, 1362, 1261, 1221, 1174, 958, 939 cm^{-1}; UV/vis (MeOH) λ_{max}/nm (log ε) 265.2 (4.35); CD (MeOH) λ_{max}/nm ($\Delta\varepsilon$) 274 (1.81), 238 (−0.92); ESI-MS(+) *m*/*z* 445.4 $[M + H]^+$, 467.3 $[M + Na]^+$, 911.6 $[2M + Na]^+$; ESI-MS(−) *m*/*z* 443.5 $[M - H]^-$; HR-ESI-MS(+) *m*/*z* 445.2593 $[M + H]^+$ (calcd for $C_{26}H_{37}O_6$, 445.2590).

Compound 9. Light-yellow oil; ^1H and ^{13}C spectroscopic data, see Table S1 in the SI; EI-MS (70 eV) *m*/*z* (%) 141 (1), 111 (100), 83 (16), 55 (36).

Reduction of Compounds 5 and 6. To a solution of **5** (1.5 mg, 0.0034 mmol) in MeOH (1 mL), excess $NaBH_4$ (1.0 mg, 0.026 mmol) was added at 0 °C, and the mixture was kept shaking for 10 min. The solvent was removed under reduced pressure, and the residue was treated with 0.1 mL of saturated NH_4Cl solution, after which 2 mL of water was added. The aqueous solution was extracted with ethyl ether (3 × 2 mL), and the combined organic layers were dried over anhydrous Na_2SO_4. After filtration and removal of the solvent, compound **5a** (1.2 mg) was obtained. In a similar procedure, compound **6** (1.7 mg, 0.0038 mmol) was transformed to **6a** (1.4 mg).

Compound 5a. CD (MeOH) λ_{max}/nm ($\Delta\varepsilon$) 286 (0.23), 270 (−0.21), 240 (1.42); ESI-MS(+) *m*/*z* 449.4 $[M + H]^+$, 920.5 $[2M + Na]^+$; ESI-MS(−) *m*/*z* 447.4 $[M - H]^-$; HR-ESI-MS(+) *m*/*z* 449.2901 $[M + H]^+$ (calcd for $C_{26}H_{41}O_6$, 449.2903).

Compound 6a. CD (MeOH) λ_{max}/nm ($\Delta\varepsilon$) 277 (−0.61), 268 (−0.56), 238 (2.30); ESI-MS(+) *m*/*z* 449.4 $[M + H]^+$, 919.6 $[2M + Na]^+$; ESI-MS(−) *m*/*z* 447.4 $[M - H]^-$; HR-ESI-MS(+) *m*/*z* 449.2901 $[M + H]^+$ (calcd for $C_{26}H_{41}O_6$, 449.2903).

Dihydroxylation of Aphadilactone A (1). To a solution of compound **1** (15 mg, 0.023 mmol) in *tert*-butyl alcohol/water (1:1, 2 mL) were added K_2OsO_4 (0.42 mg, 0.0012 mmol), $K_3Fe(CN)_6$ (112 mg, 0.34 mmol), K_2CO_3 (47 mg, 0.34 mmol), and $MeSO_2NH_2$ (11 mg, 0.12 mmol) at room temperature.[19] After about 10 h of reaction (monitored by TLC), the reaction was quenched with 5 mL of saturated $Na_2S_2O_3$. The resulting aqueous mixture was then extracted with EtOAc (3 × 10 mL). The organic phase was washed with brine (30 mL) and dried over anhydrous $MgSO_4$. After filtration, the solvent was removed in vacuo, and the residue was purified by semipreparative HPLC (CH_3CN/H_2O, 55:45 v/v) to afford **10a** (2.0 mg, t_R = 13.2 min), **11a** (2.1 mg, t_R = 14.6 min), and **12a** (2.5 mg, t_R = 7.3 min).

Compound 10a. Pale gum; $[\alpha]_D^{22}$ −4.6 (*c* 0.065, MeOH); ^1H and ^{13}C spectroscopic data, see Table S2 in the SI; UV/vis (MeOH) λ_{max}/nm (log ε) 265.4 (4.06); ESI-MS(+) *m*/*z* 695.4 $[M + H]^+$, 717.3 $[M + Na]^+$; ESI-MS(−) *m*/*z* 739.8 $[M + HCOO]^-$; HR-ESI-MS(+) *m*/*z* 717.3613 $[M + Na]^+$ (calcd for $C_{40}H_{54}O_{10}Na$, 717.3615).

Compound 11a. Pale gum; $[\alpha]_D^{22}$ −6.0 (*c* 0.05, MeOH); ^1H and ^{13}C spectroscopic data, see Table S2 in the SI; UV/vis (MeOH) λ_{max}/nm (log ε) 264.4 (3.83); ESI-MS(+) *m*/*z* 695.3 $[M + H]^+$, 717.3 $[M + Na]^+$; HR-ESI-MS(+) *m*/*z* 717.3617 $[M + Na]^+$ (calcd for $C_{40}H_{54}O_{10}Na$, 717.3615).

Compound 12a. Pale gum; $[\alpha]_D^{22}$ −21.7 (*c* 0.06, MeOH); ^1H and ^{13}C spectroscopic data, see Table S2 in the SI; UV/vis (MeOH) λ_{max}/nm (log ε) 214.2 (4.05), 265.2 (4.06); ESI-MS(+) *m*/*z* 729.4 $[M + H]^+$, 751.3 $[M + Na]^+$; ESI-MS(−) *m*/*z* 773.6 $[M + HCOO]^-$; HR-ESI-MS(+) *m*/*z* 751.3676 $[M + Na]^+$ (calcd for $C_{40}H_{56}O_{12}Na$, 751.3669).

Oxidative Cleavage of Compounds 10a−12a. Compound **10a** (1.0 mg) was dissolved in dried CH_2Cl_2 (1 mL), and a fresh batch of lead tetraacetate (1.0 mg) was slowly added at 0 °C.[20] After the raw material was completely converted (as monitored by TLC), an excess of newly prepared methanolic solution of $NaBH_4$ was added, and the reaction was continued for 10 min.[21] After workup, the resulting product was subsequently subjected to chiral HPLC analysis (chiral AD-H column, 10 mm × 250 mm, Daicel Chemical Industries, Ltd.) with *n*-hexane/isopropanol (2.7:0.3) as the mobile phase. In the same fashion, compounds **11a** (1.0 mg) and **12a** (1.2 mg) were treated, and the products were subjected to chiral HPLC analysis. As our aim was to determine the chirality of **13** by comparing its chiral HPLC retention time with those of authentic samples, the expected products

dx.doi.org/10.1021/jo402340h | J. Org. Chem. 2014, 79, 599−607

10b, **11b**, **12b** (**5a**), and **13** were not deliberately purified in the final step.

Compounds **2**–**4** (each 5 mg) were treated with a similar dihydroxylation/oxidative cleavage cascade as for **1** in a one-pot reaction to afford three final products for chiral HPLC analysis.

Synthesis of (*S*)-6-(Hydroxymethyl)-4-methyl-5,6-dihydro-2*H*-pyran-2-one (13).[18] To a solution of TBDPSiCl (9.2 g) and imidazole (2.25 g) in DMF (100 mL) was added dropwise a solution of (*R*)-oxiran-2-ylmethanol (**13a**, 2.02 g) in CH_2Cl_2 (10 mL) at 0 °C. The solution was allowed to warm to room temperature and stirred for 5 h. After workup in the normal way, the product was purified on a silica gel column (hexane/EtOAc, 50:1) to afford **13b** (8.09 g, 95%). To a slurry of CuI (95 mg) in THF (5 mL) at −30 °C was added dropwise isopropenylmagnesium bromide (0.5 M in THF, 10 mL). The thick orange mixture was stirred for 5 min, and **13b** (1.02 g) in THF (10 mL) was added dropwise. The reaction mixture was warmed to 0 °C and kept stirring for 15 min. The reaction was quenched by addition of a saturated aqueous solution of NH_4Cl (10 mL), and the mixture was worked up in the usual manner. The products were purified by column chromatography (hexane/acetone, 50:1) to yield **13c** as a colorless oil (0.98 g, 85%). To a solution of **13c** (0.92 g) in dried CH_2Cl_2 (5 mL) were added Et_3N (550 mg) and DMAP (50 mg) at 0 °C. A solution of acryloyl acid chloride (250 mg) in CH_2Cl_2 (10 mL) was then added dropwise to the reaction mixture, and stirring was continued for a further 1 h. After workup, the reaction residue was purified by silica gel column chromatography (hexane/EtOAc, 50:1) to afford **13d** (0.95 g, 90%). A solution of **13d** (250 mg) in 150 mL of dried CH_2Cl_2 was purged with dried nitrogen for 15 min, and a solution of Grubbs' catalyst II (44 mg) in 20 mL of dried CH_2Cl_2 was added dropwise under a nitrogen atmosphere. Then the reaction mixture was refluxed under a nitrogen atmosphere for 8 h. After removal of the solvent under reduced pressure, the residue was purified on a silica gel column (hexane/acetone, 20:1) to obtain **13e** (185 mg, 80%). To a solution of **13e** (52 mg) in 2 mL of THF was added TBAF (0.3 mL, 1 M in THF) at 0 °C, and stirring was continued for 0.5 h. The mixture was warmed to room temperature and kept stirring for another 2 h. After removal of the solvent in vacuo, the residue was purified by preparative TLC (chloroform/MeOH, 20:1) to afford **13** (16 mg, 80%). $[\alpha]_D^{22}$ −74.0 (*c* 0.1, MeOH); EI-MS (70 eV) *m*/*z* (%) 112 (8), 111 (100), 83 (9); HR-EI-MS *m*/*z* 111.0456 $[M - CH_2OH]^+$ (calcd for $C_6H_7O_2$, 111.0446). For ^1H and ^{13}C spectroscopic data, see Table S1 in the SI.

Synthesis of (*R*)-6-(Hydroxymethyl)-4-methyl-5,6-dihydro-2*H*-pyran-2-one (14). Except for the starting material (**14a**), the same synthetic approach and experimental conditions as used for the synthesis of **13** were applied to prepare **14**. $[\alpha]_D^{22}$ 80.0 (*c* 0.07, MeOH); EI-MS (70 eV) *m*/*z* (%) 111 (100), 94 (6), 83 (18), 82 (6), 55 (24); HR-EI-MS *m*/*z* 111.0428 $[M - CH_2OH]^+$ (calcd for $C_6H_7O_2$, 111.0446). For ^1H and ^{13}C spectroscopic data, see Table S1 in the SI.

ECD Calculations for Compounds 5–8. The ECD spectra of compounds **5**–**8** were calculated according to protocols described in the literature.[24] For details, see SI S1.

In Vitro DGAT Enzyme Inhibitory Assay. The recombinant human DGAT-1 and human DGAT-2 proteins were produced in Sf9 insect cells by a baculovirus expression system. The microsome containing DGAT enzymes was prepared as described before[1,25] and stored at −80 °C for the DGAT enzyme inhibitory assay.

The DGAT-1 inhibitory activities of compounds were measured by Phospholipid FlashPlate assays as described previously.[26] Briefly, the compounds were dissolved in DMSO and primarily tested for DGAT-1 inhibitory activity at a dosage of 10 μM with a final DMSO concentration of less than 1%. The compounds with inhibitory activities of >30% were further investigated to obtain the dose–response curves and values of IC_{50} (half of the maximal inhibitory concentration), which were calculated using GraphPad Prism 5.

The DGAT-2 inhibitory activity of compound **3** was tested by radioactive TLC assay as reported previously.[25] The radioactivity was measured using a Cyclone Plus Storage Phosphor System (PerkinElmer, cat. no. C431200).

Antimalarial Assay. Dose-dependent growth inhibition was assessed against *P. falciparum* strain Dd2 (chloroquine-resistant) using SYBR Green as described previously.[27] Briefly, ring-stage parasite cultures (200 μL/well, 1% hematocrit and 1% parasitemia) were grown for 72 h in the presence of increasing concentrations of drug. Ten-point dilutions were used to test the dose response at concentrations ranging from 5 to 0.1 μM for compound **3** and from 1 to 0.01 μM for compounds **1**, **2**, and **4**. Artemisinin was used as a positive control. Parasite growth was normalized to untreated controls. The IC_{50} calculations were performed with GraFit 5 (Erithacus Software Ltd.) using nonlinear regression curve fitting, and the reported values represent averages of two independent experiments with standard deviations.

■ ASSOCIATED CONTENT

Supporting Information

Structural determination; tabulated NMR data; ^1H, ^{13}C, and 2D NMR spectra, mass spectra, and IR spectra of **1**–**14**; DGAT inhibitions of **1**–**8**; and ECD calculation methods. This material is available free of charge via the Internet at http://pubs.acs.org.

■ AUTHOR INFORMATION

Corresponding Author

*Tel: +86-21-50806718. Fax: +86-21-50806718. E-mail: jmyue@mail.shcnc.ac.cn.

Notes

The authors declare no competing financial interest.

■ ACKNOWLEDGMENTS

Financial support for this work was provided by the National Natural Science Foundation of China (81021062, 20902095), the Foundation from the Ministry of Science and Technology of the People's Republic of China (2012CB721105), the Jeffress Memorial Trust of Virginia (J-1058), and the Virginia Commonwealth Health Research Board (208-03-12) (to M.B.C.). We thank Professor S.-M. Huang (Department of Biology, Hainan University) for the collection and identification of the plant material.

■ REFERENCES

(1) (a) Cases, S.; Smith, S. J.; Zheng, Y. W.; Myers, H. M.; Lear, S. R.; Sande, E.; Novak, S.; Collins, C.; Welch, C. B.; Lusis, A. J.; Erickson, S. K.; Farese, R. V., Jr. *Proc. Natl. Acad. Sci. U.S.A.* **1998**, *95*, 13018–13023. (b) Cases, S.; Stone, S. J.; Zhou, P.; Yen, E.; Tow, B.; Lardizabal, K. D.; Voelker, T.; Farese, R. V., Jr. *J. Biol. Chem.* **2001**, *276*, 38870–38876. (c) Yen, C. E.; Stone, S. J.; Koliwad, S.; Harris, C.; Farese, R. V., Jr. *J. Lipid Res.* **2008**, *49*, 2283–2301.

(2) Matsuda, D.; Tomoda, H. *Curr. Opin. Invest. Drugs* **2007**, *8*, 836–841.

(3) (a) Park, H. R.; Yoo, M. Y.; Seo, J. H.; Kim, I. S.; Kim, N. Y.; Kang, J. Y.; Cui, L.; Lee, C. S.; Lee, C. H.; Lee, H. S. *J. Agric. Food Chem.* **2008**, *56*, 10493–10497. (b) Oh, W. K.; Lee, C. H.; Seo, J. H.; Chung, M. Y.; Cui, L.; Fomum, Z. T.; Kang, J. S.; Lee, H. S. *Arch. Pharm. Res.* **2009**, *32*, 43–47. (c) Choi, B. W.; Lee, H. S.; Lee, K. B.; Lee, B. H. *Phytother. Res.* **2011**, *25*, 1041–1045. (d) Cui, L.; Kim, M. O.; Seo, J. H.; Kim, I. S.; Kim, N. Y.; Lee, S. H.; Park, J.; Kim, J.; Lee, H. S. *Food Chem.* **2012**, *132*, 1775–1780.

(4) Chen, S. K.; Chen, B. Y.; Li, H. In *Flora Reipublicae Popularis Sinicae (Zhongguo Zhiwu Zhi)*; Science Press: Beijing, 1997; Vol. *43*, pp 239–240.

(5) Editorial Committee of the Administration Bureau of Traditional Chinese Medicine. *Chinese Materia Medica (Zhonghua Bencao)*; Shanghai Science and Technology Press: Shanghai, 1999; Vol. *13*, p 31.

(6) Nishizawa, M.; Inoue, A.; Hayashi, Y.; Sastrapradja, S.; Kosela, S.; Iwashita, T. J. *J. Org. Chem.* **1984**, *49*, 3660−3662.
(7) (a) Wang, J. S.; Zhang, Y.; Wei, D. D.; Wang, X. B.; Luo, J.; Kong, L. Y. *Chem. Biodiversity* **2011**, *8*, 2025−2034. (b) Wang, J. S.; Zhang, Y.; Luo, J.; Kong, L. Y. *Magn. Reson. Chem.* **2011**, *49*, 450−457. (c) Zhang, Y.; Wang, J. S.; Wei, D. D.; Wang, X. B.; Luo, J.; Luo, J. G.; Kong, L. Y. *Phytochemistry* **2010**, *71*, 2199−2204. (d) Liu, Q. A.; Chen, C. J.; Shi, X. A.; Zhang, L.; Chen, H. J.; Gao, K. *Chem. Pharm. Bull.* **2010**, *58*, 1431−1435.
(8) (a) Polonsky, J.; Varon, Z.; Arnoux, B.; Pascard, C.; Pettit, G. R.; Schmidt, J. H.; Lange, L. M. *J. Am. Chem. Soc.* **1978**, *100*, 2575−2576. (b) Polonsky, J.; Varon, Z.; Arnoux, B.; Pascard, C.; Pettit, G. R.; Schmidt, J. M. *J. Am. Chem. Soc.* **1978**, *100*, 7731−7733.
(9) Miller, L. H.; Ackerman, H. C.; Su, X. Z.; Wellems, T. E. *Nat. Med.* **2013**, *19*, 156−167.
(10) (a) Saxena, S.; Pant, N.; Jain, D. C.; Bhakuni, R. S. *Curr. Sci.* **2003**, *85*, 1314−1329. (b) Wells, T. N. *Malar. J.* **2011**, *10* (Suppl. 1), S3.
(11) World Health Organization, Division of Control of Tropical Diseases. Report CTD/MAL/97.20; World Health Organization: Geneva, 2001.
(12) (a) Burrows, J. N. *Future Med. Chem.* **2012**, *4*, 2233−2235. (b) Burrows, J. N.; van Huijsduijnen, R. H.; Möhrle, J. J.; Oeuvray, C.; Wells, T. N. *Malar. J.* **2013**, *12*, 187.
(13) Palacpac, N. M.; Hiramine, Y.; Seto, S.; Hiramatsu, R.; Horii, T.; Mitamura, T. *Biochem. Biophys. Res. Commun.* **2004**, *321*, 1062−1068.
(14) Palacpac, N. M. Q.; Hiramine, Y.; Mi-ichi, F.; Torii, M.; Kita, K.; Hiramatsu, R.; Horii, T.; Mitamura, T. *J. Cell Sci.* **2004**, *117*, 1469−1480.
(15) Chimichi, S.; Boccalini, M.; Cosimelli, B.; Viola, G.; Vedaldi, D.; Dall'Acqua, F. *Tetrahedron Lett.* **2002**, *43*, 7473−7476.
(16) Leslie, A. K.; Li, D. D.; Koide, K. *J. Org. Chem.* **2011**, *76*, 6860−6865.
(17) Harada, N.; Nakanishi, K. In *Circular Dichroic Spectroscopy: Exciton Coupling in Organic Stereochemistry*; University Science Books: Mill Valley, CA, 1983.
(18) (a) Hansen, T. V. *Tetrahedron: Asymmetry* **2002**, *13*, 547−550. (b) Trost, B. M.; Amans, D.; Seganish, W. M.; Chung, C. K. *J. Am. Chem. Soc.* **2009**, *131*, 17087−17089. (c) Inoue, M.; Nakada, M. *J. Am. Chem. Soc.* **2007**, *129*, 4164−4165. (d) Yadav, J. S.; Hossain, S. S.; Madhu, M.; Mohapatra, D. K. *J. Org. Chem.* **2009**, *74*, 8822−8825.
(19) Kolb, H. C.; VanNieuwenhze, M. S.; Sharpless, K. B. *Chem. Rev.* **1994**, *94*, 2483−2547.
(20) Gelmi, M. L.; Nava, D.; Leone, S.; Pellegrino, S.; Baldelli, E.; Zunino, F.; Cappelletti, G.; Cartelli, D.; Fontana, G. *J. Org. Chem.* **2008**, *73*, 8893−8900.
(21) Luo, X. Y.; Zhou, Z. Q.; Li, X.; Liang, X. M.; Ye, J. X. *RSC Adv.* **2011**, *1*, 698−705.
(22) He, X. F.; Wang, X. N.; Fan, C. Q.; Gan, L. S.; Yin, S.; Yue, J. M. *Helv. Chim. Acta* **2007**, *90*, 783−791.
(23) Zhang, H. J.; Luo, J.; Shan, S. M.; Wang, X. B.; Luo, J. G.; Yang, M. H.; Kong, L. Y. *Org. Lett.* **2013**, *15*, 5512−5515.
(24) (a) Yuan, T.; Zhu, R. X.; Zhang, H.; Odeku, O. A.; Yang, S. P.; Liao, S. G.; Yue, J. M. *Org. Lett.* **2010**, *12*, 252−255. (b) Zhu, Q.; Tang, C. P.; Ke, C. Q.; Li, X. Q.; Liu, J.; Gan, L. S.; Weiss, H. C.; Gesing, E. R.; Ye, Y. *J. Nat. Prod.* **2010**, *73*, 40−44.
(25) Qian, Y. M.; Wertheimer, S. J.; Ahmad, M.; Cheung, A. W. H.; Firooznia, F.; Hamilton, M. M.; Hayden, S.; Li, S. M.; Marcopulos, N.; McDermott, L.; Tan, J.; Yun, W. Y.; Guo, L. A.; Pamidimukkala, A.; Chen, Y. S.; Huang, K. S.; Ramsey, G. B.; Whittard, T.; Conde-Knape, K.; Taub, R.; Rondinone, C. M.; Tilley, J.; Bolin, D. *J. Med. Chem.* **2011**, *54*, 2433−2446.
(26) Zhao, G.; Souers, A. J.; Voorbach, M.; Falls, H. D.; Droz, B.; Brodjian, S.; Lau, Y. Y.; Iyengar, R. R.; Gao, J.; Judd, A. S.; Wagaw, S. H.; Ravn, M. M.; Engstrom, K. M.; Lynch, J. K.; Mulhern, M. M.; Freeman, J.; Dayton, B. D.; Wang, X. J.; Grihalde, N.; Fry, D.; Beno, D. W. A.; Marsh, K. C.; Su, Z.; Diaz, G. J.; Collins, C. A.; Sham, H.; Reilly, R. M.; Brune, M. E.; Kym, P. R. *J. Med. Chem.* **2008**, *51*, 380−383.
(27) Smilkstein, M.; Sriwilaijaroen, N.; Kelly, J. X.; Wilairat, P.; Riscoe, M. *Antimicrob. Agents Chemother.* **2004**, *48*, 1803−1806.